



### **Science Arts & Métiers (SAM)**

is an open access repository that collects the work of Arts et Métiers Institute of Technology researchers and makes it freely available over the web where possible.

This is an author-deposited version published in: <https://sam.ensam.eu>  
Handle ID: <http://hdl.handle.net/10985/8233>

#### **To cite this version :**

Clément BARTHES, Khalid M. MOSALAM, Nazih MECHBAL, Marc RÉBILLAT - Structural health monitoring of high voltage electrical switch ceramic insulators in seismic areas - In: 7th European Workshop on Structural Health Monitoring, France, 2014-07-08 - Proceedings of the 7th European Workshop on structural Health Monitoring - 2014

Any correspondence concerning this service should be sent to the repository

Administrator : [scienceouverte@ensam.eu](mailto:scienceouverte@ensam.eu)



# STRUCTURAL HEALTH MONITORING OF HIGH VOLTAGE ELECTRICAL SWITCH CERAMIC INSULATORS IN SEISMIC AREAS

Marc Rébillat<sup>1</sup>, Clément B. Barthes<sup>2</sup>, Nazih Mechbal<sup>1</sup>, Khalid M. Mosalam<sup>2</sup>

<sup>1</sup> DYSCO, PIMM, Arts et Métiers ParisTech, France

<sup>2</sup> PEER, University of California Berkeley, CA, USA

marc.rebillat@ensam.eu, clementbarthes@berkeley.edu

## ABSTRACT

High voltage electrical switches are crucial components to restart rapidly the electrical network right after an earthquake. But there currently exists no automatic procedure to check if these ceramic insulators have suffered after an earthquake, and there exists no method to recertify a given switch. To deploy a vibration-based structural health monitoring method on ceramic insulators a large shake table able to generate accelerations up to 3 g was used. The idea underlying the SHM procedure proposed here is to monitor the apparition of cracks in the ceramic insulators at their early stage through the change of the resonant frequency of the first mode of the structure and the non-linearity that they generate in its dynamic response. The Exponential Sine Sweep Method is used to estimate a nonlinear model of the structure under test from only one dynamic measurement. A classic linear damage index (DI) based on the variation of the frequency of the first mode is compared to an original nonlinear one using the ratio of the amplitudes of the third harmonic and the fundamental frequency. Results show that both DIs increase monotonically with the number of solicitations, thus validating the use of the nonlinear DI. It is also shown that the nonlinear DI presented here seems more sensitive than the linear one.

**KEYWORDS :** *Structural health monitoring, ceramic materials, nonlinear approach.*

## 1. INTRODUCTION

High voltage electrical switches, see Fig. 1(a), are crucial components to restart rapidly the electrical network right after an earthquake. Indeed, they could be used immediately after an earthquake to turn off the electrical network in damaged substations and to restore power in undamaged ones. Such switches must thus fulfill strong requirements to be deployed in seismic areas such as California. Even so, the ceramic insulators (Fig. 1(a)) constitute a very fragile part of these switches. There currently exists no automatic procedure to check if these ceramic insulators have suffered after an earthquake, and no automatic method to recertify a given switch. As a consequence, all of the ceramic insulators are generally replaced after an earthquake event, even the healthy ones. Hence the electrical network cannot restart quickly. To avoid doing so, automatic procedures able to detect damage and quantify its amount without any human intervention are needed [1, 2].

Structural health monitoring (SHM) is an emerging technology designed to automate the inspection process undertaken to assess the health condition of structures [3]. In a smart structure, SHM systems may automatically process data and assess the condition of the structure. Several techniques may be used depending on the structure's material, the technology used for acting and sensing, the position, the size, and the nature of damage [4]. Among other things, we can highlight vibration-based approaches which have the advantage of being sensitive to small flaws and of offering the capability to monitor significant areas with few sensors [5, 6]. To deploy a vibration-based structural health monitoring method on ceramic insulators, these need to be equipped with sensors. In the present work, accelerometers were chosen for sensing. The ceramic insulators were also excited at their base in order to check their dynamic response but also to induce fatigue damage.

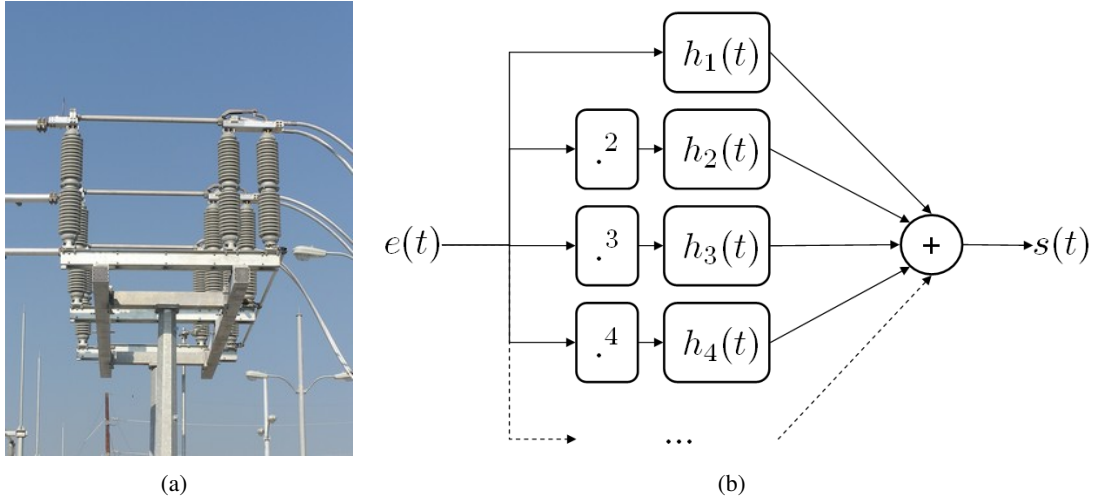


Figure 1 : a) Electrical switch (161 kV / 2 kA) from Southern States with ceramic insulators (source: <http://www.southernstatesllc.com>). b) A cascade of Hammerstein models.

It is assumed here that fatigue damage in ceramic insulators consists of cracks that grow before the final breakage of the insulator. The idea underlying the SHM procedure is to monitor the growth of these cracks during the early stage through the diminution of the frequency of the first mode of the structure [7] and through the non-linearities that they generate in the dynamic response [8]. This is done by using an original vibration-based structural health monitoring approach previously developed by the authors [9–11]. For this, we assume that a ceramic insulator can be modeled as a cascade of Hammerstein models as shown in Fig. 1(b). The Exponential Sine Sweep Method [9, 12] is then used to estimate a nonlinear model of the ceramic insulator from only one dynamic measurement. A classic linear damage index based on the variation of the frequency of the first mode is then compared to an original nonlinear one based on the amplitude of the third harmonic. Results show that both damage indexes increase monotonically with the number of solicitations, thus validating the use of the nonlinear DI. It is also shown that the nonlinear damage index presented here appears to be more sensitive than the linear one.

The paper is organized as follows. The way the damage indexes are built from an estimated nonlinear model is first described in Sec. 2. Then, the experimental procedure used to test the ceramic insulators is presented in Sec. 3. The obtained results are finally given in Sec. 4. and a conclusion is drawn in Sec. 5.

## 2. DAMAGE INDEXES BUILT FROM AN ESTIMATED NONLINEAR MODEL

### 2.1 Chosen nonlinear model: cascade of Hammerstein models

In a cascade of Hammerstein system, each branch is composed of one nonlinear static polynomial element followed by a linear one  $h_n(t)$  as shown in Fig. 1(b). The relation between the input  $e(t)$  and the output  $s(t)$  of such a system is given by Eq. (1) where “ $(*)$ ” denotes the convolution operator.

$$s(t) = \sum_{n=1}^N (h_n * e^n)(t) \quad (1)$$

Any cascade of Hammerstein models is fully represented by its kernels  $\{h_n(t)\}_{n \in \{1 \dots N\}}$ , which are only a set of linear filters. This model is thus quite simple to use and intuitive to understand.

## 2.2 Exponential sine sweeps

Estimating each kernel  $h_n(t)$  of a cascade of Hammerstein models is not a straightforward task. A simple estimation method that has been proposed previously by the authors [9] for this purpose is briefly recalled here. To experimentally cover the frequency range over which the system under study has to be identified, cosines with time-varying frequencies are commonly used. When the instantaneous frequency of  $e(t) = \cos[\phi(t)]$  is increasing exponentially from  $f_1$  to  $f_2$  in a time interval  $T$ , this signal is called an “*Exponential Sine Sweep*”. It can be shown [9, 12] that by choosing  $T = (2m - \frac{1}{2}) \frac{\ln(f_2/f_1)}{2f_1}$  with  $m \in \mathbb{N}^*$ , one obtains:

$$\forall k \in \mathbb{N}^* \quad \cos[k\phi(t)] = \cos[\phi(t + \Delta t_k)] \quad \text{with} \quad \Delta t_k = \frac{T \ln(k)}{\ln(f_2/f_1)} \quad (2)$$

Eq. (2) states that for any exponential sine sweep of duration  $T$ , multiplying the phase by a factor  $k$  yields to the same signal, advanced in time by  $\Delta t_k$ .

## 2.3 Kernel recovery in the time domain

If an exponential sine sweep is presented at the input of a cascade of Hammerstein models, by combining Eq. (2) and Eq. (1) we obtain the following relation:

$$s(t) = \sum_{n=1}^N (\gamma_n * e)(t + \Delta t_n) \quad \text{with} \quad \gamma_n(t) = \sum_{k=1}^n c_{k,n} h_k(t) \quad (3)$$

where  $\gamma_n(t)$  is the contribution of the different kernels to the  $n^{\text{th}}$  harmonic. In order to identify each kernel  $h_n(t)$  separately, a signal  $y(t)$  operating as the inverse of the input signal  $e(t)$  in the convolution sense can be built as shown in [9]. After convolving the output of the cascade of Hammerstein models  $s(t)$  given in Eq. (3) with  $y(t)$ , one obtains Eq. (4):

$$(y * s)(t) = \sum_{n=1}^N \gamma_n(t + \Delta t_n) \quad (4)$$

Because  $\Delta t_n \propto \ln(n)$  and  $f_2 > f_1$ , the higher the order of non-linearity  $n$ , the more advanced is the corresponding  $\gamma_n(t)$ . Thus, if  $T_m$  is chosen long enough, the different  $\gamma_n(t)$  do not overlap in time and can be separated by simply windowing them in the time domain. Using Eq. (5), the family  $\{h_n(t)\}_{n \in [1, N]}$  of the kernels of the cascade of Hammerstein models under study can then be fully extracted. Details of the computation of the matrix  $C$  are provided in [9].

$$[h_1(t) \dots h_N(t)]^T = C [\gamma_1(t) \dots \gamma_N(t)]^T \quad (5)$$

## 2.4 Damage indexes definition

### 2.4.1 Classic damage index

As a first approximation, the effect of the growth of the crack in the structure under study can be modeled as a local decrease of its stiffness. Thus, as the crack grows, the overall stiffness of the structure will decrease as well as the frequency of its first mode. Let  $f_H$  be the frequency of the first mode of the structure in the healthy case and  $f_D$  the same frequency in the damaged case. These frequencies can here be easily extracted from the estimated nonlinear model as the kernel  $h_1(t)$ , or its Fourier transform  $H_1(f)$ , is nothing else than the linear response of the system. After the analysis of  $H_1(f)$  in a healthy and a damaged cases, we can then define a classic linear damage index as [7]:

$$DI_L = \frac{f_D - f_H}{f_H} \quad (6)$$

### 2.4.2 Original nonlinear damage index

The dynamic response of a breathing crack alternates between the open and closed phases and its behavior is not the same in each of these two phases. The dynamic response of a crack appearing in a ceramic insulator is thus nonlinear by nature, and is expected to exhibit mainly odd harmonics for symmetry reasons [8]. Furthermore, the amount of non-linearity generated by the crack in the dynamic response of the structure should also be proportional to its size. For an arbitrary frequency  $f$ , the odd harmonics contained in the dynamic response of the system can here be easily extracted from the estimated nonlinear model as the Fourier transform of the kernels  $\{H_1(f), H_3(3f), H_5(5f), H_7(7f), \dots\}$  are nothing else than the amplitudes of the fundamental frequency and its odd harmonics. Let  $f_H$  be the frequency of the first mode of the structure in the healthy case and  $f_D$  the same frequency in the damaged case. By denoting  $R_3(f)$  the ratio of the amplitude of the third harmonic to the amplitude of the fundamental in the neighborhood  $[f - \delta f, f + \delta f]$  of the frequency  $f$ , a second original nonlinear damage index  $DI_{NL}$  can then be built as:

$$R_3(f) = \int_{f-\delta f}^{f+\delta f} \left| \frac{H_3(3v)}{H_1(v)} \right| dv \quad \text{and} \quad DI_{NL} = \frac{R_3(f_D) - R_3(f_H)}{R_3(f_H)} \quad (7)$$

## 3. EXPERIMENTAL PROCEDURE

### 3.1 The PEER shaking table

The UC Berkeley 6 axes hydraulic shake table was used for this experiment [1]. The shake table dimensions are 6 m×6 m. The maximum displacement is  $\pm 13$  cm horizontally and  $\pm 5$  cm vertically. The maximum acceleration in each direction is 3 g and the maximum velocity is 1 m/sec. A hydraulic shake table does not have a constant frequency response, and the dynamic properties of the specimen will change this response. Furthermore, in hydraulic systems servo-valves have a nonlinear response, clevises compliance vary in tension and compression, and minor backlash may be present. All of these nonlinear events generate odd harmonics which can be problematic for this experiment since the damage index  $DI_{NL}$  defined in Eq. (7) relies on an estimated nonlinear model of the specimen. Oftentimes a correction technique consists of building frequency response model of the table beforehand with a non-destructive random excitation then invert this function to obtain a constant frequency response. But this technique can only correct linear errors. So for harmonic signals it is preferred to use close loop compensators which are more prone to instability but are also more powerful. An amplitude-phase controller (APC) monitors the amplitude and phase error of the linear part and updates an error correction. An adaptive harmonic canceler (AHC) corrects the most repeatable non-linearities in the table response by sending signals with the same frequency and opposite polarity. It must be noted that the correction parameters of the APC and the AHC are required to adapt to the varying frequency of the exponential sine sweep signal. A high sweep rate may lead to control instability, hence it was preferred to use a slow rate of *1 oct/min*.

### 3.2 Ceramic insulators and associated instrumentation

The ceramic insulator consists of two posts spliced in the center, manufactured by PPC insulators, as shown in Fig. 2(b). The ceramic is tapered, with a base diameter of 172 mm and a top diameter of 137 mm (without the rain sheds). These insulators (height: 4 m, weight: 450 kg) are commonly used on 500 kV disconnect switches, with two stacks holding the switch hinge and one stack holding the

jaw where the switch blade sits in the closed position. While fairly simple, these disconnect switches must operate properly after an earthquake because they must be opened prior to any maintenance work in the electric substation. Despite their brittle properties, ceramic insulators are often preferred over fiberglass insulators because they do not require to be filled with insulating oil or SF6 gas. A numerical analysis of the specimen was performed in order to assess the expected strain at various levels, see Fig. 2(a). The model is linear elastic, and the boundary conditions between the various elements were modeled as bonded. A static analysis was performed, with gravity load applied in the horizontal direction. As expected, the maximum longitudinal stress was observed at the base, where the specimen was expected to fail. The specimen was equipped with two strain gauges at its base and with two 3-axis accelerometers placed at mid-height and at the top of the structure, see Fig. 2(b).

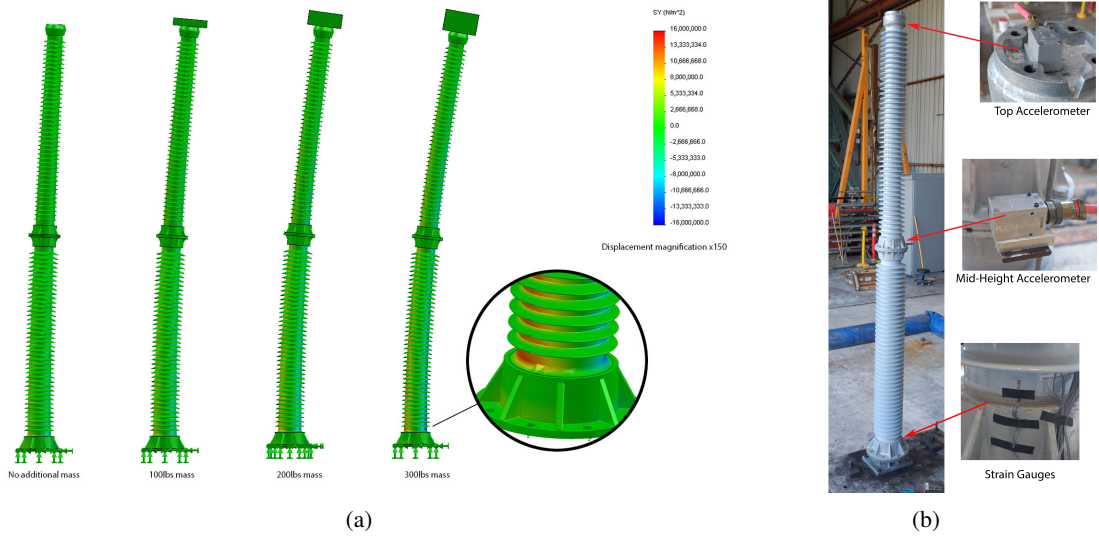


Figure 2 : a) Numerical analysis of the specimen subjected to gravity load along the vertical plane. b) Specimen on the shake table, instrumented with two strain gauges at its base and with two 3-axis accelerometers placed at mid-height and at the top of the structure.

### 3.3 Earthquakes used for damage generation and excitation signal

The earthquake signals used in this experiment are the signals prescribed in IEEE-693 [13]. Two different earthquake amplitudes were used: 1.0 g and 1.5 g. The response spectra of these earthquakes is represented in Fig. 3(a). During the experiment, the table response always enveloped these targeted response spectra. The specimen was subjected to a total of 15 earthquake signals. After each earthquake signal, an exponential sine sweep was performed sequentially in each direction of the table ( $x$  and  $y$ -directions). This excitation signal is an exponential sine sweep with  $f_1 = 0.7$  Hz,  $f_2 = 50$  Hz,  $T = 364.4$  s and an amplitude of 0.1 g. Time history signals were acquired with a sampling frequency of  $f_s = 200$  Hz. In order to induce more damage, mass was added during the test. This added mass was always removed during the exponential sine sweeps. The different earthquake levels are sorted in Table 3(b) based on their severity. Based on the exponential sine sweep response of the specimen, it was decided to either increase the severity level or keep it constant. Most of the damage was observed for the severity indexes 6 and 7. The specimen failed near its base, as expected in Sec. 3.2, during the sixteenth earthquake.

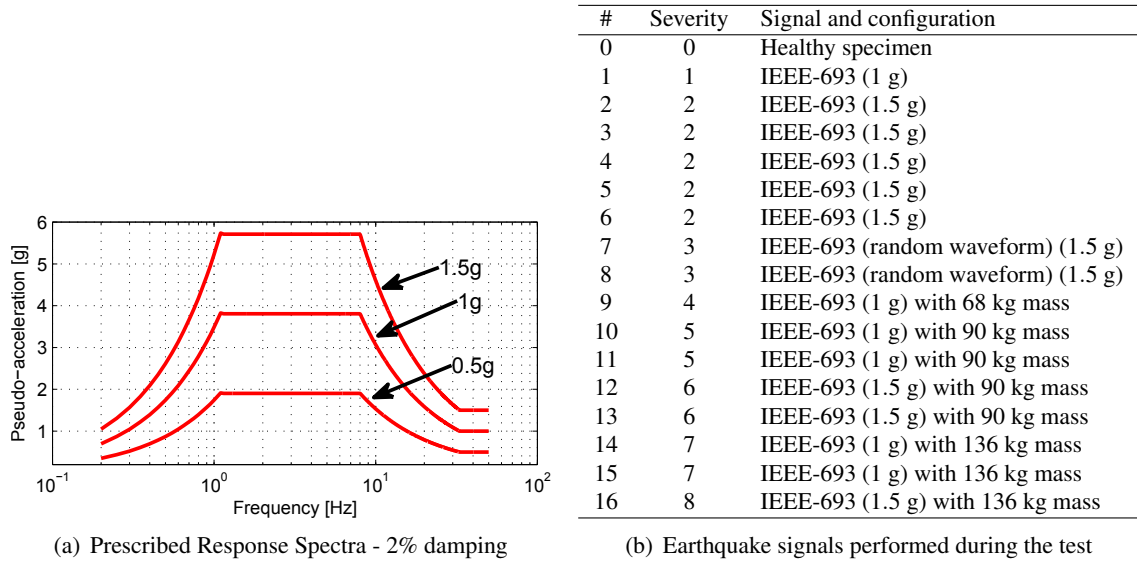


Figure 3 : Earthquakes used for damage generation

## 4. RESULTS

### 4.1 Evolution of the estimated kernels with damage

A nonlinear model of the specimen under test up to a nonlinear order  $N = 4$  was estimated by means of the procedure described in Sec. 2. fed with the signals obtained in Sec. 3. from each available sensor. The amplitude of the Fourier transform of the different kernels as a function of the severity index defined in Tab. 3(b) is shown in Fig. 4(a) for the y-axis of the mid-height accelerometer subjected to an exponential sine sweep in the y-direction, see Fig. 2(b).

From Fig. 4(a) it can be noted that the amplitude of the different kernels does not exhibit variation during the damage process. This variation is mainly observed near the resonant frequency of the first mode for  $H_1(f)$  and near the corresponding harmonics for the higher level kernels. By looking at Fig. 4(b) which is a zoomed version of Fig. 4(a) near the frequency of the first mode for  $H_1(f)$  and the frequency of the third harmonic for  $H_3(f)$  it can be seen that the effects that have been qualitatively described in Sec. 2.4 are here experimentally observed. Indeed, when considering  $|H_1(f)|$ , it can be seen that the resonant frequency of the first mode of the structure under test is decreasing with the severity index thus validating the softening phenomenon. Furthermore, when looking at both  $|H_1(f)|$  and  $|H_3(f)|$ , one can observe that the third harmonic amplitude increases while the fundamental amplitude decreases with the severity index validating the fact that the structure response becomes more and more nonlinear as damage increases [8].

### 4.2 Damage index variations with severity index

Two damage indexes were built from the nonlinear models estimated after each earthquake. A classic linear one  $DI_L$  based on the variation of the frequency of the first mode defined by Eq. (6), and an original nonlinear one  $DI_{NL}$  based on the ratio of the amplitudes of the third harmonic and the fundamental frequency defined by Eq. (7). For  $DI_{NL}$ , the parameter  $\delta f$  was set to 0.01 Hz, meaning that the amplitude ratio is averaged in a neighborhood of 0.01 Hz near the resonant frequency and the third harmonic. The variations of both damage indexes with the number of earthquakes are plotted in Fig. 5 for the x-axis of the mid-height accelerometer when subjected to an exponential sine sweep in the x-direction and for a strain gauge when subjected to an exponential sine sweep in the y-direction.

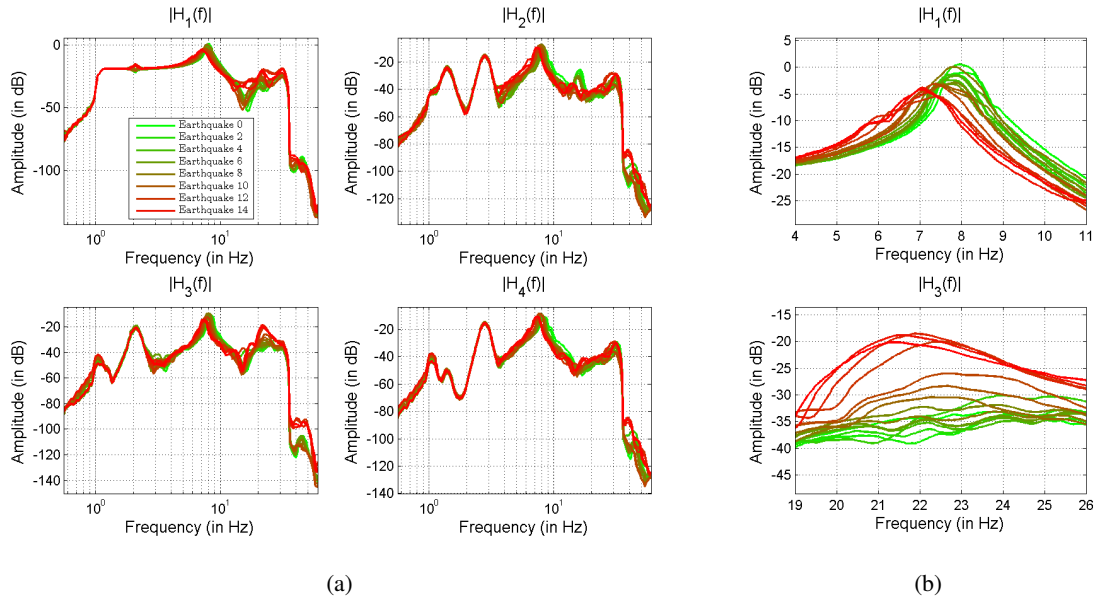


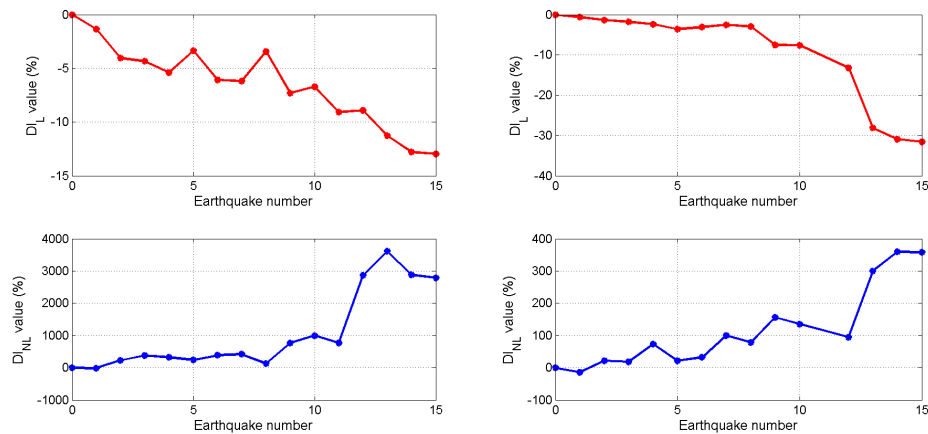
Figure 4 : Amplitude of the Fourier transform of the different kernels of the  $x$ -axis of the mid-height accelerometer subjected to an exponential sine sweep in the  $x$ -direction, see Fig. 2(b), as a function of the severity index: a) overview b) zoom near the fundamental and the third harmonics. Colors are coding the earthquake number given in Tab. 3(b) as partially indicated by the legend.

From Fig. 5, it can be seen that when the severity index increases, the linear damage index  $DI_L$  monotonically decreases while the nonlinear one  $DI_{NL}$  monotonically increases. This is consistent with the theoretical expectations of Sec. 2.4. Furthermore one can notice that the trends provided by both  $DI$ s are consistent (*i.e.* there is not one  $DI$  that increases greatly while the other one is not), thus validating  $DI_{NL}$  with respects to  $DI_L$  that is already well documented in the literature and expected to be reliable. Finally it can be seen that  $DI_{NL}$  varies by almost 4000 % during the damaging process while  $DI_L$  varies by only 30 %. Thus it appears that the nonlinear damage index  $DI_{NL}$  is more sensitive than the linear damage index  $DI_L$ .

## 5. CONCLUSION

A vibration-based structural health monitoring (SHM) procedure was tested on ceramic insulators with a large shake table. The idea behind the SHM procedure proposed here was to monitor the growth of cracks in the ceramic insulators at their early stages through the change of the resonant frequency of the first mode of the structure and the non-linearities that they generate in its dynamic response. The Exponential Sine Sweep Method was used to estimate a nonlinear model of the structure under test from only one dynamic measurement. A classic linear damage index  $DI_L$  was compared to an original nonlinear damage index  $DI_{NL}$ . This preliminary experiment showed that  $DI_{NL}$  can quantify damage induced by earthquakes in ceramic insulators. Its behavior is consistent with the behavior of the classic  $DI_L$ . Furthermore, since the proposed  $DI_{NL}$  appears to vary more than the  $DI_L$ , future work should focus on the ability to detect damage that cannot be detected by  $DI_L$ . Future experiments should include the use of a shaker pot able to produce higher frequencies than a shake table in order to study the behavior of high order harmonics. In addition, the amplitude of the damage index varied greatly based on the instrument location. The mid-height accelerometers and the base level strain gauges were more adequate to assess damage than the top accelerometers. It is planned to investigate the underlying cause of these differences in order to deploy the sensors more efficiently.





(a) Mid-height accelerometer, x-axis, exponential (b) Strain gage, y-axis, exponential sine sweep in sine sweep in the x-direction.

Figure 5 : Variations of the classic linear damage index  $DI_L$  defined by Eq. (6) and of an original nonlinear one  $DI_{NL}$  defined by Eq. (7) with the severity index.

## REFERENCES

- [1] A. S. Whittaker, G. L. Fenves, A. S. J. Gilani, Seismic evaluation and analysis of high-voltage substation disconnect switches, *Engineering Structures* 29 (12) (2007) 3538–3549.
- [2] F. Paolacci, R. Giannini, Seismic reliability assessment of a high-voltage disconnect switch using an effective fragility analysis, *Journal of Earthquake Engineering* 13 (2) (2009) 217–235.
- [3] K. Worden, C. R. Farrar, G. Manson, G. Park, The fundamental axioms of structural health monitoring, *Proceedings of the Royal Society A: Mathematical, Physical and Engineering Science* 463 (2082) (2007) 1639–1664.
- [4] B. Balageas, P. Fritzen, C., A. Gemes, *Structural Health Monitoring*, Wiley-ISTE, 2006.
- [5] C. R. Farrar, S. W. Doebling, D. A. Nix, Vibration-based structural damage identification, *Philosophical Transactions of the Royal Society of London Series A-mathematical Physical and Engineering Sciences* 359 (1778) (2001) 131–149.
- [6] Z. Q. Su, L. Ye, Y. Lu, Guided lamb waves for identification of damage in composite structures: A review, *Journal of Sound and Vibration* 295 (3-5) (2006) 753–780.
- [7] O. Salawu, Detection of structural damage through changes in frequency: a review, *Engineering Structures* 19 (9) (1997) 718 – 723.
- [8] M. I. Friswell, J. E. T. Penny, Crack modeling for structural health monitoring, *Structural Health Monitoring* 1 (2) (2002) 139–148.
- [9] M. Rébillat, R. Hennequin, E. Corteel, B. F. G. Katz, Identification of cascade of Hammerstein models for the description of nonlinearities in vibrating devices, *Journal of Sound and Vibration* 330 (5) (2011) 1018–1038.
- [10] M. Rébillat, R. Hajrya, N. Mechbal, Detection of structural damage using the exponential sine sweep method, in: *Proceedings of the International workshop on Structural Health Monitoring*, 2013.
- [11] M. Rébillat, R. Hajrya, N. Mechbal, Nonlinear structural damage detection based on cascade of hammerstein models, *Mechanical Systems and Signal Processing* (in press). doi:http://dx.doi.org/10.1016/j.ymssp.2014.03.009.
- [12] A. Novak, L. Simon, F. Kadlec, P. Lotton, Nonlinear system identification using exponential swept-sine signal, *IEEE Transactions On Instrumentation and Measurement* 59 (8) (2010) 2220–2229.
- [13] IEEE, 693-2005 - IEEE Recommended Practice for Seismic Design of Substations (2005).